

Effect of Surface Coating on Electrochemical Properties of Rare Earth-Based AB₅-type Hydrogen Storage Alloys

Danyang Xie

Hebei Key Laboratory of Applied Chemistry, College of Environmental and Chemical Engineering, Yanshan University, Qinhuangdao 066004, China
E-mail: xiedanyang1997@163.com

Received: 23 June 2016 / Accepted: 9 September 2016 / Published: 10 October 2016

In our endeavor to improve overall electrochemical properties of AB₅-type alloys, we performed an electroless plating on the alloy surface. X-ray diffraction shows that the bulk structure is not changed via coating, however, scanning electron microscopy results show that particle shape Ni-coating and flake shape Co-coating adhere tightly to the alloy surface. The electrochemical tests show that initial activation is greatly improved as activation number reduces from 9 (untreated) to 5 (Ni-coated) and 3 (Co-coated). The surface coating improves the charge transfer rate at surface, enlarging hydrogen concentration between in the bulk and at the surface, and therefore promotes the hydrogen diffusion rate process. Consequently, the high rate dischargeability is ameliorated. At a discharge current density 1200 mA/g, HRD increases from 48.6% to 61.0% and 60.9% for Ni-coating and Co-coating alloy, respectively. The coating layer provides a protective function to the alloy surface and leads to an increase in cycling stability. After charge /discharge for 200 cycles, the capacity retention increases from 63% (untreated) to 71% (Ni-coated) and 73% (Co-coated), respectively.

Keywords: Hydrogen storage alloys; Surface coating; Rare earth-based alloys; Electrochemical properties; Kinetics

1. INTRODUCTION

Metal hydride/nickel (MH/Ni) batteries have been widely used in portable electric devices and electric hand tools owing to their high power characteristics and environmental friendliness [1, 2]. Rare earth-based AB₅-type hydrogen storage alloys which usually consist of rare earth elements and transition metal elements in the atomic ratio of 1:5, as the initially commercialized type of alloys possess considerable market share in negative electrode materials of MH/Ni batteries. The AB₅-type alloys have some advantages, such as easy activation and long cycle life, and are now widely used in

MH/Ni batteries. However, this type of alloys is suffered from low discharge capacity, and their high rate dischargeability needs an improvement in order to meet the requirement from high-power MH/Ni batteries. Therefore it is significant to improve overall electrochemical properties of AB₅-type alloys [3-6].

In recent years, plenty of investigations report methods to improve electrochemical properties. Diaz et al. [7, 8] used 2wt.% molybdenum in AB₅ alloys, and found a decrease in charge transfer resistance. Shen et al. [9] found Al benefited to cycling stability improvement. Fe and Mn were also found to be beneficial in improving electrochemical properties [10, 11]. Carbon-based materials, nanotubes modified surface of AB₅-type alloys, catalyzed hydrogen anodic reaction and helped to improve the electrochemical properties [12, 13]. Young et al. [14] performed a gas atomization to Cu-containing AB₅ metal hydride alloys, and improved the cycling stability while kept a high low temperature dischargeability for the electrodes. Besides gas atomization, preparing thin films is another method for improve electrochemical properties [15].

The electrochemical properties were characterized in electrode process, which is a series of reactions occurred in the interface between electrode and electrolyte. And therefore the morphology and properties of the alloy surface contributed a great share to the overall electrochemical properties [16, 17]. In order to obtain more suitable surface for electrochemical reactions, surface treatment was widely applied to get high catalytic surface. Zhao et al. [18] got a F-0.5%Pd-LaNi_{4.25}Al_{0.75} alloy by combination of fluorination and palladium deposition, and discovered a excellent hydrogen storage property. Besides combined treatment, single fluorination was reported to be an effective method [19, 20]. Microencapsulation of alloy powders with metallic or alloy coatings such as Ni-P, Pd, Cu, Co were reported to improving the catalytic activity and high-rate dischargeability owing to the effect of transition metal on hydrogen reaction catalysis [21-23]. Polymer coating was also recently reported to improve the electrochemical properties owing to functional groups which help in hydrogen transferring [24].

In order to improve catalytic activity at the alloys surface, Co and Ni are coated at the surface, and the effects of metallic layer on microstructure and electrochemical properties are investigated.

2. EXPERIMENTAL

2.1 Surface treatment

The Rare earth-based AB₅-type alloy was prepared by arc melting. The ingots were mechanically crashed into powders of -300 mesh for microstructure characterization and surface treatments. The surface treatment was performed via an electroless plating method. The plating solution composition is as below: 0.05 mol/L NiSO₄ (or CoSO₄), 0.05 mol/L glycine. The alloy powders were first etched with 0.001 mol/L HCl solution, and then merged into the plating solution with stirring for 5 min. Finally, a 0.05 mol/L NaBH₄ solution was added into the mixed solution and stirred for another 20 min. The treated powders were dried at 60°C under vacuum.

2.2 Electrochemical tests

0.30 g alloy powders between 200-400 mesh and 0.10 g carbonyl nickel powders were mixed with 2 drops of 3 wt.% PVA (poly vinyl alcohol) solution. A nickel foam with a size of 2×2 cm was used as a substrate to load the mixture for preparing an electrode. The pasted electrodes were dried in vacuum at 60°C for 4 h, and then cold pressed under 10 MPa.

Electrochemical tests were performed in a tri-electrode system, with metal hydride (MH) working electrode, Hg/HgO reference electrode and Ni(OH)₂/NiOOH counter electrode. A 6 mol/L KOH solution was used as the electrolyte. All the charge/discharge processes were performed on a DC-5 battery testing instrument at a constant temperature 293 K. The working electrode was charged at 60 mA/g for 8 h followed by a 10 min rest and then discharged at the same current density. The electrochemical tests were measured on a CHI660D working station. The linear polarization curves of the electrodes by scanning electrode potential at a rate of 0.1 mV/s from -5 to 5 mV (vs. open-circuit potential) at 50% depth of discharge (DOD), while 5 mV/s from 0 to 1500 mV (vs. open circuit potential) for the anodic polarization curve at 50% DOD. Electrochemical impedance spectra (EIS) measurements were conducted at 50% depth of discharge (DOD), in the frequency range of 1 MHz to 0.1 Hz with AC amplitude of 5 mV.

2.3 Microstructure characterization

Phase structure was analyzed by X-ray diffraction (XRD) on a PC-2500/MAX X-ray diffractometer. Surface morphology of alloy powders was observed on a HITACHIS-4800 scanning electron microscopy (SEM) linked with energy dispersive spectroscopy (EDS).

3. RESULTS AND DISCUSSION

3.1 Microstructure characterization

Fig.1 shows XRD patterns of the alloy powders with and without surface coating. The three alloys all consist mainly of CaCu₅-type phase (PDF #65-0093). No diffraction peaks corresponding to Ni or Co is detected, which is ascribed to small amount of Ni and Co coated on the surface. The results show that surface coating method in our study does not change the main phase structure of the CaCu₅-type phase alloy. However, the diffraction peaks shift a little, especially the two peaks at $2\theta = 40^\circ$ and 67° . As NaBH₄ was added into the plating solution, H⁻ ions appeared. Some of them reacted with Ni²⁺ or Co²⁺ to get the modifying layer, and some reacted with H⁺ in the solution to form H₂. The H₂ molecules near the alloy could be dissociated and absorbed into the alloy bulk in the form of hydrogen atoms, and the ones far from alloy would release from the solution, which could be found as the hydrogen bubbles after NaBH₄ was added. The hydrogen atoms then got out of the alloy during alloy drying at 60°C under vacuum. However, the lattices could not recover completely when the hydrogen atoms were released from the alloy. The absorption/ desorption of the hydrogen atoms may cause

distortion of the lattices as well as change of some interplanar spacing in the CaCu_5 -type phase, and consequently leads to a small shift of the diffraction peaks [25].

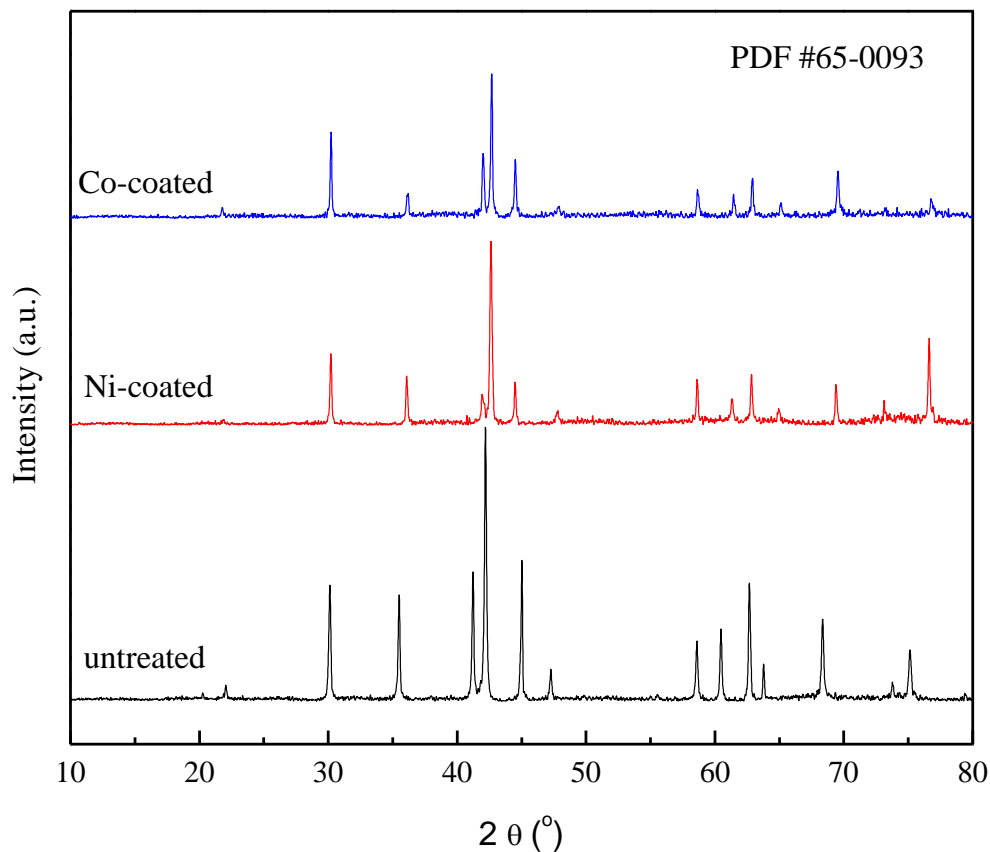


Figure 1. XRD patterns for alloy powders before and after surface coating

For the surface microstructure characterization we used scanning electron microscopy, and the resulted images are shown in Fig.2. In Fig.2 (a), the surface of the untreated alloy is smooth. Some small particles from the mechanical ground step attached to the bulky alloy particles. In Fig.2 (b) a uniform Ni coating layer is found at the alloy surface, and on the edge the coating layer is thicker than the other area. EDS results show that Ni content obviously increases. For the Co-coated alloy powders (in Fig.2 (c)) flake-like coating layer is found at the alloy surface, and EDS results also show increase in Co content. Under the existence of amino acetic acid as complex agent, Ni- and Co-coating deposition on the alloy powders may follow the steps below: At first, the complex agent amino acetic acid was adsorbed onto the alloy surface owing to the complexation between oxygen element and rare earth element. And then the coated elements, Ni and Co come near to the $-\text{NH}_2$ and complexed with the nitride element. Finally, as reductant NaBH_4 was added, Ni and Co deposit onto the alloy surface.

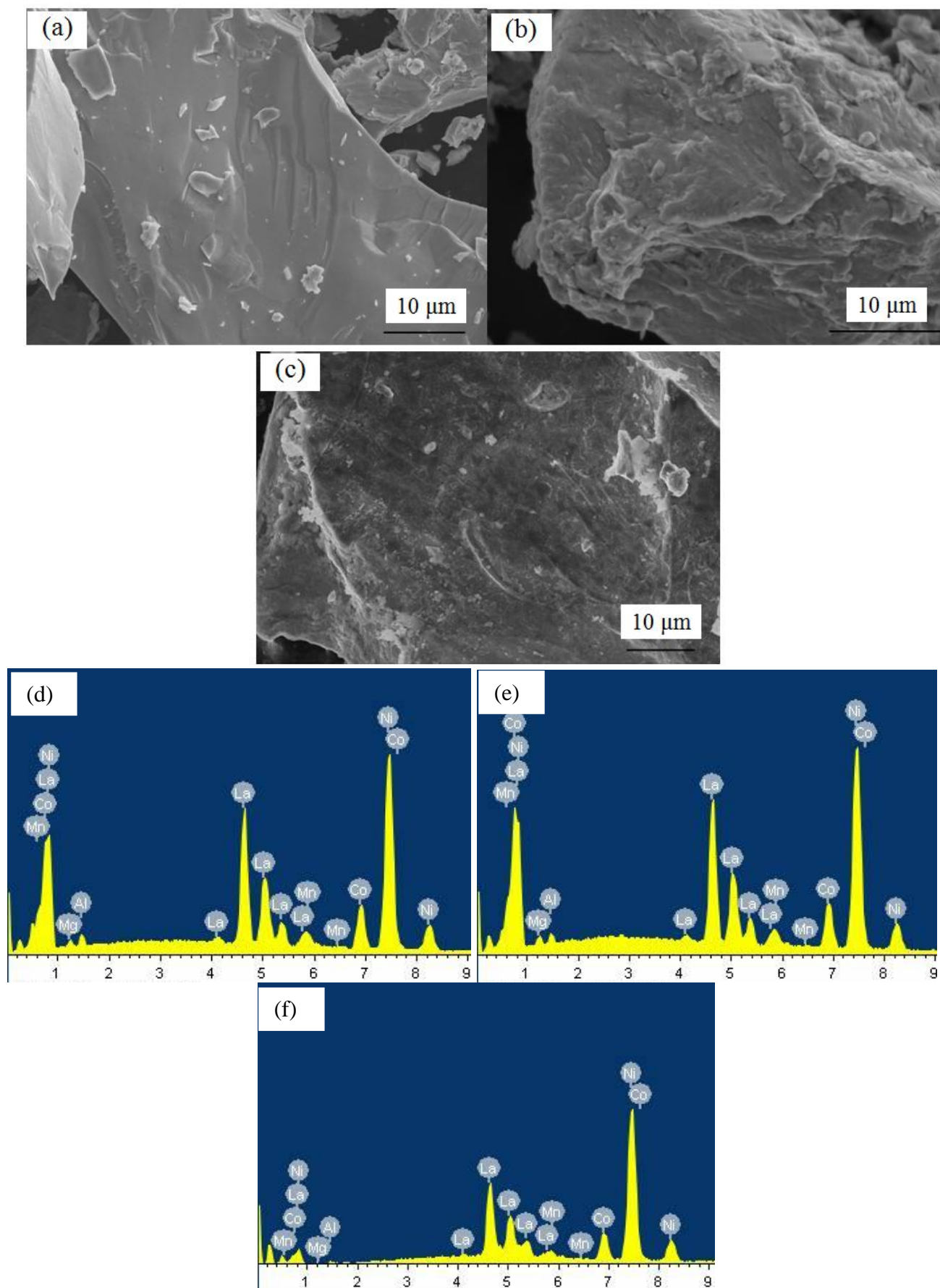


Figure 2. SEM images and EDS analysis of the alloy powders before and after coating treatments (a)(d) untreated alloy; (b)(e) Ni-coated alloy; (c)(f) Co-coated alloy

3.2 Discharge properties

In the initial charge/discharge stage, discharge capacity increases with cycle number as shown in Fig.3. This stage is called activation for the electrode. In this stage the hydrogen atoms enter/ release from the alloy lattices until the lattices become large enough for suitable hydrogen atom storage. For the untreated alloy electrode, it need 9 cycles for activation, while the activation cycle number for surface coated alloy electrode is reduced to 5 and 3 for the Ni-coated and Co-coated electrode, respectively. The similar activation cycle reduction has been reported in other surface treatment studies [26]. After Ni- or Co-coating, native oxide passive layer is removed and the metallic coating surface possesses high electric-activity. It makes the polarization be suppressed in electrochemical reaction, and hydrogen be released completely from the alloy lattices. The complete hydrogen release facilitates sufficient expanse/contraction of lattices, and thereby the activation becomes easier after surface coating [27]. After activation a maximum discharge capacity appears for each electrode. There is not any obvious change in maximum discharge capacity for the coating species, for Ni and Co are not hydrogen absorbed or electro-active.

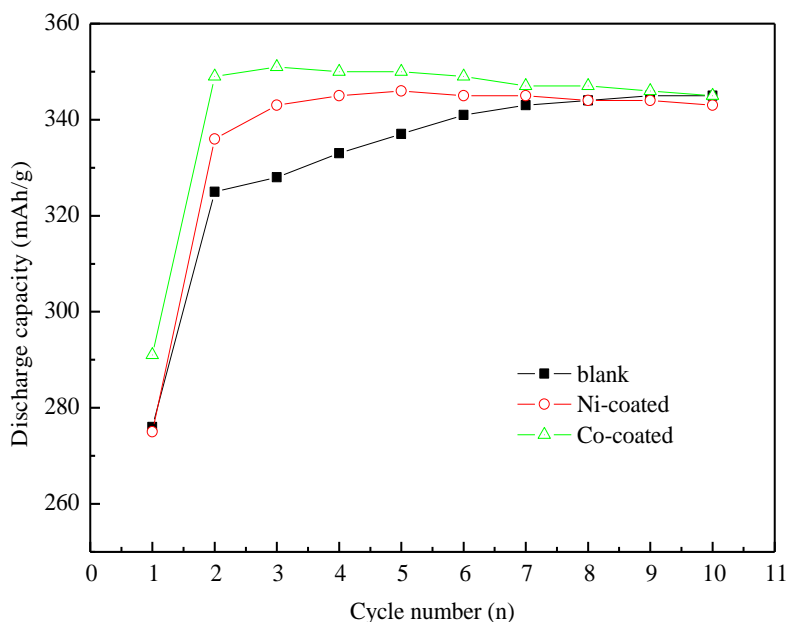


Figure 3. Activation curves of alloy electrodes with and without surface coating

Fig.4 shows discharge capacity vs. cycle number. The discharge capacity decreases with increasing cycle number. However, discharge capacity of electrodes with surface coating decreases slowly. At the 200th cycle, the untreated alloy electrode keeps 63% of its maximum discharge capacity, while it remains 71% and 73% for the Ni-coated and Co-coated alloy electrode, respectively.

Oxidation is a very important reason for capacity degradation. The elements with low surface energy, such as rare earth elements in AB₅-type alloys are easily to be oxidized and form coarse hydroxides RE(OH)₃ (RE denotes rare earth elements), which causes chemical composition changes in

the alloy and consequently capacity degradation. Besides chemical composition changes, the formed hydroxides are usually loose and even provides pathway for the alkaline solution to contact with the fresh sub-surface. Subsequently, new hydroxides formed and more electrochemical capacity is lost [5,28]. The coating metallic layer, Ni and Co is relatively passive in alkaline solution, not easy to be oxidized into hydroxides, compared with rare earth elements. As well as they deposit as a denser and protective layer at the alloy surface, preventing direct contact between alloy surface and alkaline electrolyte. Thereby the degradation is remarkably suppressed owing to reduced oxidation, and the cycling stability is greatly improved.

The high rate dischargeability (HRD) is a key important parameter to characterize the kinetic properties. HRD is defined as a ratio of discharge capacity at a specific discharge current density to a discharge capacity at 60 mA/g. The HRD values are shown in Fig.5. It is found discharge capacity decreases at higher current density, while the HRD is improved after surface coating. At the discharge current density 1200 mA/g, HRD increases from 48.6% to 61.0% and 60.9% for Ni-coated and Co-coated alloy, respectively. It is well known that HRD is controlled by bulk diffusion and surface reaction for the alloy electrode. After surface coating, the surface reaction is faster owing to high catalytic activity of the coating layer, and following faster reaction promotes the diffusion. Consequently, kinetics is improved and thereby HRD are remarkably ameliorated. Below we use electrochemical impedance spectra (EIS), linear polarization and anodic polarization to testify our speculation.

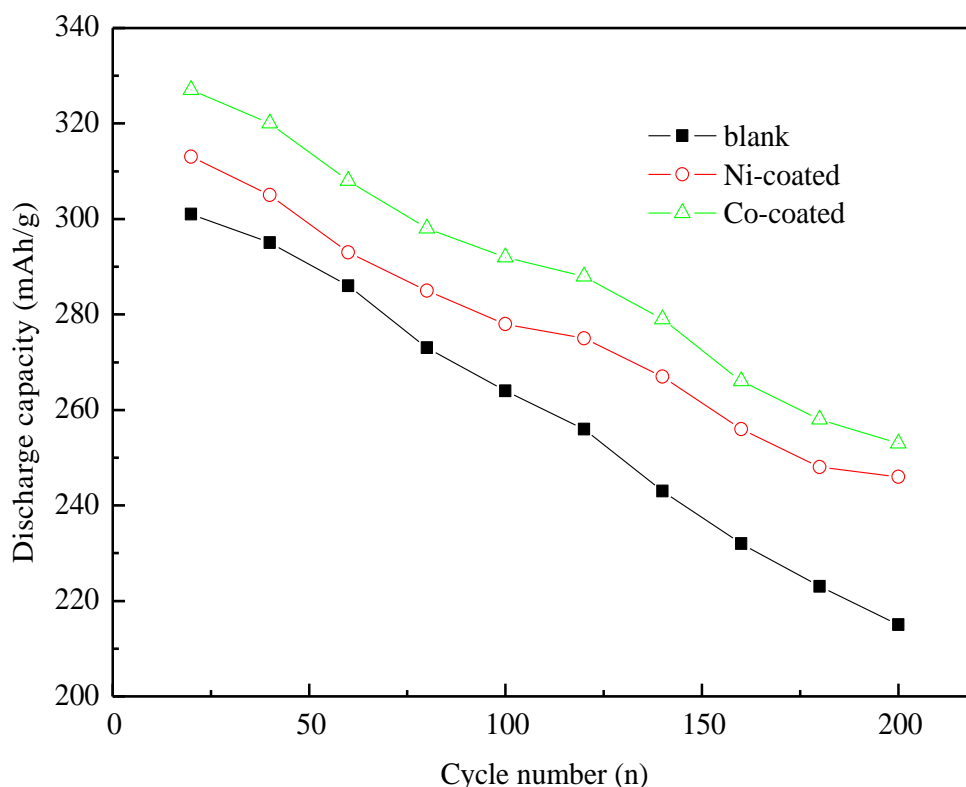


Figure 4. Discharge capacity of alloy electrodes with and without surface coating

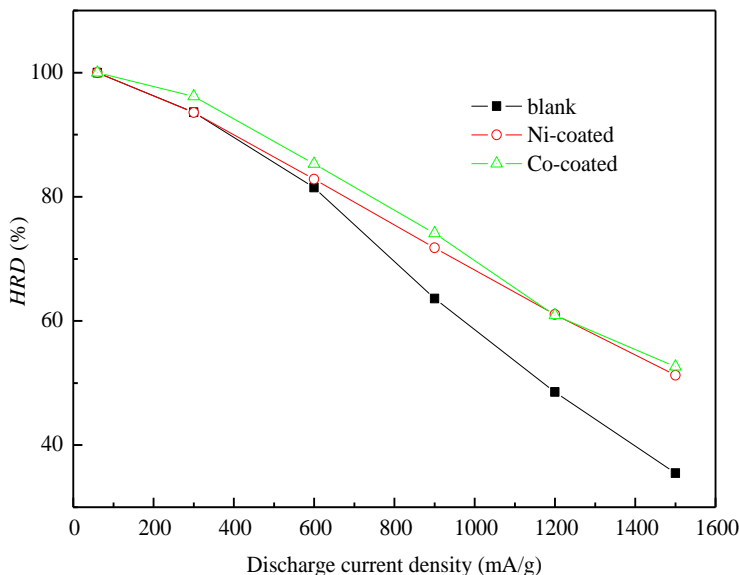


Figure 5. High rate dischargeability of the bare, Co-coated and Ni-coated alloy electrodes

3.3 Kinetic characteristics

The kinetic tests were carried out to study change in surface charge transferring rate and bulk hydrogen diffusion rate. Fig.6 shows the EIS of alloy electrodes with and without surface coating. Each spectrum consist of a semi-circle in high frequency range corresponding to the electrode resistance and a straight line in low frequency range corresponding to hydrogen diffusion [29]. As is written previously the preparation for testing electrode is the same between different one, and so the contact resistance may show little differences between each other. Therefore, it can be considered that the difference in radius of semi-circle results from the electrochemical reaction.

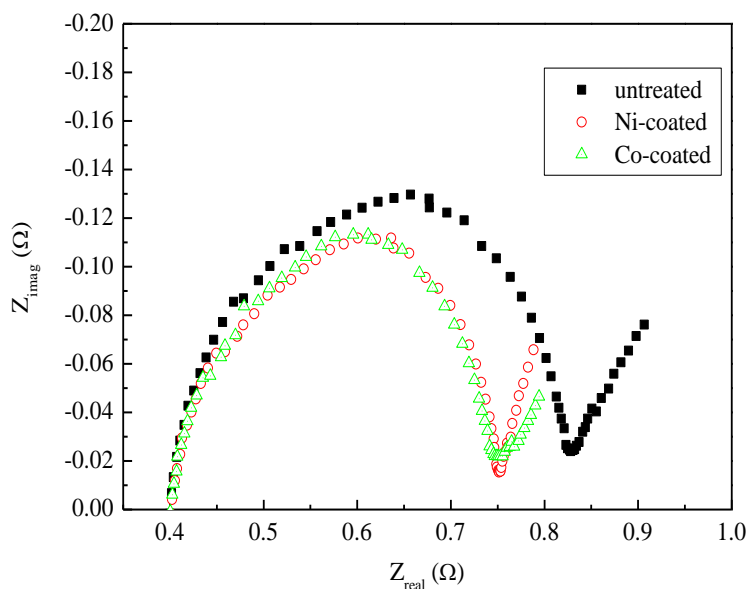


Figure 6. EIS of alloy electrodes with and without surface coating at 50% DOD

The radius of the semi-circle after surface coating Ni and Co, the radius of the semi-circle decreases remarkably. That is charge transfer resistance decreases after Ni- and Co-coating. Ni- and Co-coating improve electro-catalytic activity at the alloy surface and thereby make the charge transfer easier and faster.

Fig. 7 presents a complete contrast of the linear polarization curves of alloy electrodes. The exchange current density can be calculated by the following equation [30]:

$$I_0 = RTI/F\eta$$

where I_0 is the exchange current density, mA/g; R is the gas constant, J/mol/K; T is the absolute temperature, K; F is the Faraday constant, C/mol. The calculated results show that the exchange current density increases from 306.1 mA/g (untreated) to 371.3 mA/g (Ni-coated) and 380.2 mA/g (Co-coated), respectively. The Ni- and Co-coated alloy electrodes show superior exchange current density to untreated alloy electrode. The larger exchange current density indicates higher electro-catalytic activity after surface coating.

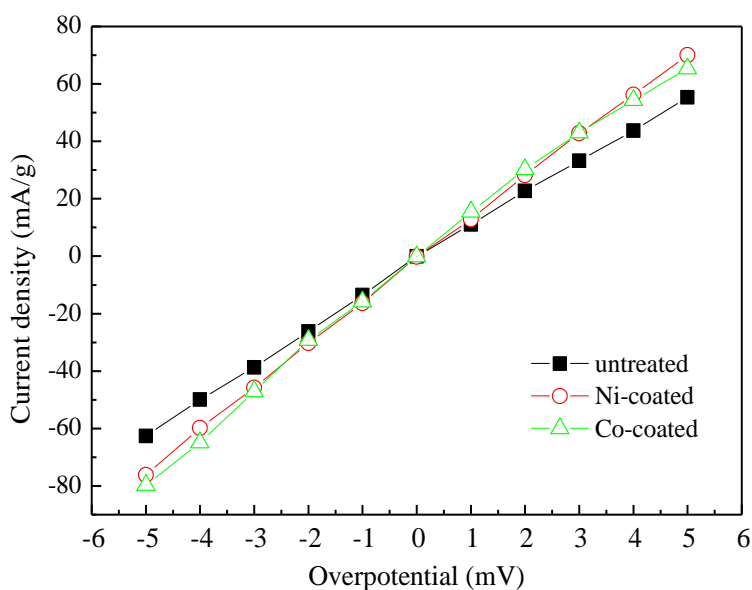


Figure 7. Linear polarization curves of alloy electrodes with and without surface coating at 50% DOD

Fig. 8 shows anodic polarization curves of alloy electrodes with and without surface coating. With increase of overpotential, hydrogen atom oxidation at the surface becomes easier until hydrogen concentration at surface becomes zero. And a peak current value at the curve, limiting current density I_L which characterizes the hydrogen diffusion rate appears. The surface coating increases the I_L value from 2563 mA/g to 3213 mA/g (Ni-coated) and 3440 mA/g (Co-coated), respectively. It is considered as the Ni- and Co-coating at the surface leads to an increase in charge transfer rate at the surface, reducing hydrogen concentration at the surface, and thereby promoting the hydrogen diffusion in alloy bulk under a larger concentration difference [31].

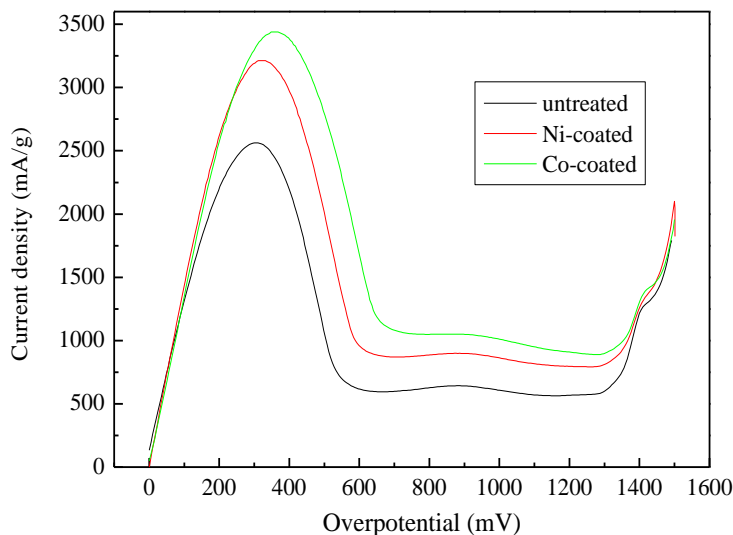


Figure 8. Anodic polarization curves of alloy electrodes with and without surface coating at 50%DOD

From the electrochemical kinetics tests, it is found that charge transfer rate at the surface and hydrogen diffusion rate in the bulk are both improved, and consequently the high rate dischargeability is greatly improved.

4 CONCLUSIONS

The rare earth-based AB₅-type alloys were treated via an electroless plating Ni and Co layer method. The surface coating does not change the phase structure, however, particle shape Ni-coating and flake shape Co-coating is found at the treated alloy surface, respectively. The coating Ni and Co layers have high electro-catalytic activity during hydrogen anodic electrode process, and thereby improve the electrochemical properties. After surface coating the activation number for electrodes reduces from 9 to 5 (Ni-coated) and 3 (Co-coated). The high rate dischargeability is greatly improved at larger discharge current density, and it increases from 48.6% to 61.0% and 60.9% for Ni-coated and Co-coated alloy at a discharge current density of 1200 mA/g, respectively. The improvement in kinetics is caused by higher catalytic activity at the surface, shown as a smaller charge transfer resistance and a higher exchange current density, as well as a faster diffusion rate in the bulk owing to a larger hydrogen concentration difference after surface coating. The coating layer is able to keep the alloy surface from corrosion, and consequently improves the cycle stability.

ACKNOWLEDGEMENTS

This work was financially supported by the National Natural Science Foundation of China (NO. 21303157).

References

1. Y. Li, S. Han and Z. Liu, *Int. J. Hydrog. Energy*, 35 (2010) 12858.
2. G. Kuang, Y. Li, F. Ren, M. Hu and L. Lei, *J. Alloy Compd.*, 605 (2014) 51.
3. Z. Ma, W. Zhou, C. Wu, D. Zhu, L. Huang, Q. Wang, Z. Tang and Y. Chen, *J. Alloy Compd.*, 660 (2016) 289.
4. X. Han, W. Wu, X. Bian, X. Liu, L. Huang and J. Wu, *Int. J. Hydrog. Energy*, 41 (2016) 7445.
5. X. Shang, S. Lu, X. Peng, Y. Fan, B. Zhang, Z. Zhang and B. Liu, *Int. J. Electrochem. Sci.*, 9 (2014) 4913.
6. X. Shang, S. Lu, Z. Zhang, Y. Fan and B. Liu, *Int. J. Electrochem. Sci.*, 9 (2014) 3078.
7. V. Diaz, R. Humana, E. Teliz, F. Ruiz, E. Castro, R. Faccio and F. Zinola, *Int. J. Hydrog. Energy*, 40 (2015) 6639.
8. V. Diaz, E. Teliz, F. Ruiz, P.S. Martinez, R. Faccio and F. Zinola, *Int. J. Hydrog. Energy*, 38 (2013) 12811.
9. R. Shen, H. Zhou, T. Chen, Q. Yao, J. Deng, Z. Wang and S. Li, Proceedings of the 2015 3rd International Conference on Machinery, Materials and Information Technology Applications, China, 2015, 1580.
10. J.-Y. Kim, C.-N. Park, J.-S. Shim, C.-J. Park, J. Choi and H. Noh, *J. Power Source*, 180 (2008) 648.
11. M. Tliha, C. Khaldi, H. Mathlouthi, J. Lamloumi and A. Percheron-Guegan, *J. Alloy Compd.*, 440 (2007) 323.
12. H. Zhang, Y. Chen, G. Zeng, H. Huang, Z. Xie and X. Jie, *Mater. Sci. Eng. A*, 464 (2007) 17.
13. L.A. Benavides, D.J. Cuscueta and A.A. Ghilarducci, *Int. J. Hydrog. Energy*, 40 (2015) 4925.
14. K. Young, T. Ouchi, A. Banik, J. Koch, M.A. Fetcenko, L.A. Bendersky, K. Wang and M. Vaudin, *J. Alloy Compd.*, 509 (2011) 4896.
15. C.Y.V. Li, Z.M. Wang, S. Liu and S.L.I. Chan, *J. Alloy Compd.*, 456 (2008) 407.
16. T. Bai, S. Han, X. Zhu, Y. Zhang, Y. Li and W. Zhang, *Mater. Chem. Phys.*, 117 (2009) 173.
17. S. Yang, H. Liu, S. Han, Y. Li and W. Shen, *App. Surf. Sci.*, 271 (2013) 210.
18. B.T. Zhao, L.F. Liu, Y.M. Ye, S.L. Hu, D. Wu and P.Z. Zhang, *Int. J. Hydrog. Energy*, 41 (2016) 3465.
19. Z.J. Ji, Z.M. Wang, J.Q. Deng, Q.R. Yao and H.Y. Zhou, *Rus. J. Electrochem.*, 51 (2015) 244.
20. Y. Chen, Y. Chen, D. Zhu, C. Wu and D. Chao, *Rare Met. Mater. Eng.*, 42 (2013) 905.
21. M. Li, Y. Zhu, C. Yang, J. Zhang, W. Chen and L. Li, *Int. J. Hydrog. Energy*, 40 (2015) 13949.
22. L. Sun, J. Lin, Z. Cao, F. Liang and L. Wang, *J. Alloy Compd.*, 650 (2015) 15.
23. L. Sun, J. Lin, F. Liang, Z. Cao and L. Wang, *Mater. Lett.*, 161 (2015) 686.
24. L. Hu, J. Li and W. Yang, *Ionics*, 21 (2015) 3209.
25. X. Zhang, M. Zhao, W. Yin, Y. Chai, *Mater. Sci. Eng. B*, 117 (2005) 123.
26. Y. Li, Y. Tao, D.D. Ke, Y.F. Ma and S.M. Han, *Appl. Surf. Sci.* 357 (2015) 1714.
27. X.Y. Zhao, L.Q. Ma, Y. Ding, Y. Meng and X.D. Shen, *Int. J. Hydrog. Energy*, 34 (2009) 3506.
28. C.Y. Ni, H. Y. Zhou, Z. M. Wang, Q. R. Yao and L.Y. Lu, *Int. J. Electrochem. Sci.*, 9 (2014) 2397.
29. X. Wang, H. Hao, J. Liu, T. Huang and A. Yu, *Electrochim. Acta*, 11 (2011) 4065.
30. L. Zhang, S. Han, Y. Li, S. Yang, X. Zhao and J. Liu, *J. Electrochem. Soc.*, 161 (2014) A1844.
31. X. Zhao, L. Ma, Y. Gao, Y. Ding and X. Shen, *Int. J. Hydrog. Energy*, 34 (2009) 1904.